Water Research X 25 (2024) 100268

Contents lists available at ScienceDirect

Water Research X

journal homepage: www.sciencedirect.com/journal/water-research-x

Efficient and sustainable removal of linear alkylbenzene sulfonate in a membrane biofilm: Oxygen supply dosage impacts mineralization pathway

Ting Wei, Ting Ran, Weikang Rong, Yun Zhou *

College of Resources and Environment, Huazhong Agricultural University, Wuhan, 430070, China

ARTICLE INFO

Keywords:
Linear alkylbenzene sulfonate
Membrane aerated biofilm reactor
Oxygen supply
Mineralization and denitrification
Biomineralization pathway

ABSTRACT

Linear alkylbenzene sulfonate (LAS) can be thoroughly mineralized within sufficient oxygen (O_2), but which is energy intensive and may causes serious foaming problem. Although cometabolism can achieve efficient LAS removal within a wide range of O_2 dosages, how O_2 dosage systematically affects LAS metabolic pathway is still unclear. Here, membrane aerated biofilm reactor (MABR) enabled accurate O_2 delivery and bulk dissolved oxygen (DO) control. MABR achieved efficient removal of LAS (>96.4 %), nitrate (>97.8 %) and total nitrogen (>96.2 %) at the three target DO conditions. At high DO condition (0.6 mg/L), LAS was efficiently removed by aerobic mineralization (predominant) coupled with aerobic denitrification biodegradation with the related functional enzymes. *Pseudomonas, Flavobacterium, Hydrogenophaga*, and *Pseudoxanthomonas* were dominant genus contributing to four possible LAS aerobic metabolic pathways. As O_2 dosage reduced to only 29.7 % of the demand for LAS mineralization, O_2 facilitated LAS activation, benzene-ring cleavage and a portion of respiration. NO_3^--N respiration-induced anaerobic denitrification also contributed to ring-opening and organics mineralization. *Desulfomicrobium* and *Desulfonema* related two possible anaerobic metabolic pathways also contributed to LAS removal. The findings provide a promising strategy for achieving low-cost high LAS-containing greywater treatment.

1. Introduction

Linear alkylbenzene sulfonate (LAS) is the most commonly used synthetic anionic surfactant in household detergents and personal care products, which contributes to the majority of organics (60–80 %) in greywater (Mungray and Kumar 2009; Kim et al., 2021). LAS fundamental structure consists of a sulfophenyl polar head (hydrophilic) and nonpolar dodecane alkyl chain tail (hydrophobic) (Jensen 1999). Low LAS dosage (< 0.1 g g^{-1} TSS) has negligible effects on denitrifying microorganisms (Elsgaard 2010), but high concentration of LAS (>0.1 g g^{-1} TSS) will aggregate into micelles in the aqueous phase (Zhou et al. 2019), which improve cell membrane permeability and even cause cell lysis (Zhou et al. 2020a; Zhou et al. 2020b). High LAS-containing greywater in the aquatic environment will adversely impact microbial activity and system stability during biological treatment (Zhou et al. 2019). Thus, the elimination of LAS is crucial for sustainable development of ecological environment and human society.

LAS can be rapidly and almost completely biodegraded (>98 %) under aerobic conditions (Babaei et al. 2019). LAS biodegradation is normally initiate with ω-oxidation of the alkyl chain and β-oxidation of the C_2 fragments (Mungray and Kumar 2009; Swisher 1986). The cleavage of aromatic ring in the sulfophenyl carboxylic acids (SPCs) produced during these oxidation processes that enabling full LAS mineralization (Perales et al. 2003). However, aerobic LAS aeration biodegradation is energy intensive due high amounts of required oxygen (O_2) (Liu et al. 2018a), and traditional direct aeration may cause serious foaming problem (Zhang et al. 2023). The complete mineralization of LAS under anoxic or anaerobic conditions has not been previously discussed. Limited information indicated that 79 % of LAS can be converted to SPCs intermediates in anoxic marine sediments (Lara-Martín et al. 2007). Anaerobic microbes can use LAS as sulfur source (Denger and Cook 1999) or carbon and energy source (Motteran et al. 2018) under insufficient sulfur or carbon conditions, respectively. Anaerobic LAS biodegradation may also occur if the inoculum is obtained from aerobic environments (compost and activated sludge from a wastewater treatment plant) (Angelidaki et al. 2000). Results indicated that O_2 concentration is a key factor that affects LAS metabolism (Garcia et al. 2005; Gejlsbjerg et al. 2004).

* Corresponding author.
E-mail address: yzhou112@mail.hzau.edu.cn (Y. Zhou).

https://doi.org/10.1016/j.wroa.2024.100268
Received 29 September 2024; Received in revised form 14 October 2024; Accepted 20 October 2024
Available online 24 October 2024

The membrane aerated biofilm reactor (MABR) exhibits unique advantages in achieving accurate gas supply for microbial metabolism, which includes hollow fiber membrane based bubbleless aeration, high O_2 delivery and utilization rates (Rittmann 2006). MABR can effectively treat high LAS-containing greywater (Zhou et al. 2020b), with treatment efficiency remaining stable even when dissolved oxygen (DO) is reduced to 0.38 ± 0.02 mg/L (Zhou et al. 2020c). Reducing O_2-supply capacity to 20 % of the demand for complete benzene biodegradation in MABR, aerobic activation, cleavage, and denitrification related respiration enabled efficient co-removal of benzene and N (Liu et al. 2018a). Chemical oxygen demand (COD) to total nitrogen (TN) ratio of 20 g g^{-1} achieved highest removal of LAS and N due to the improved related microbes and enzymes functional for LAS mineralization and N reduction in an O_2 based MABR (Zhou et al. 2021a). High ammonia monooxygenase levels enabled the cometabolism of ammonia oxidation and LAS mineralization in the MABR, and achieved efficient co-removal of LAS and N under insufficient O_2 conditions (Zhou et al. 2021b). Despite the increased application of MABR in simultaneous removal of LAS and N at different DO conditions, little is known about how O_2 supply concentration affects LAS metabolic pathways in the MABR.

In this study, MABR was applied for accurate O_2 delivery and DO control. Dynamics of LAS metabolic pathway were assessed under different O_2 supply capacities with nitrate as nitrogen source in the MABR. LAS and nitrogen removal, dissolved organic matters (DOM) characteristics, microbial community succession and potential related functional enzymes were at tracked at different DO concentrations (0.0, 0.3 and 0.6 mg/L).

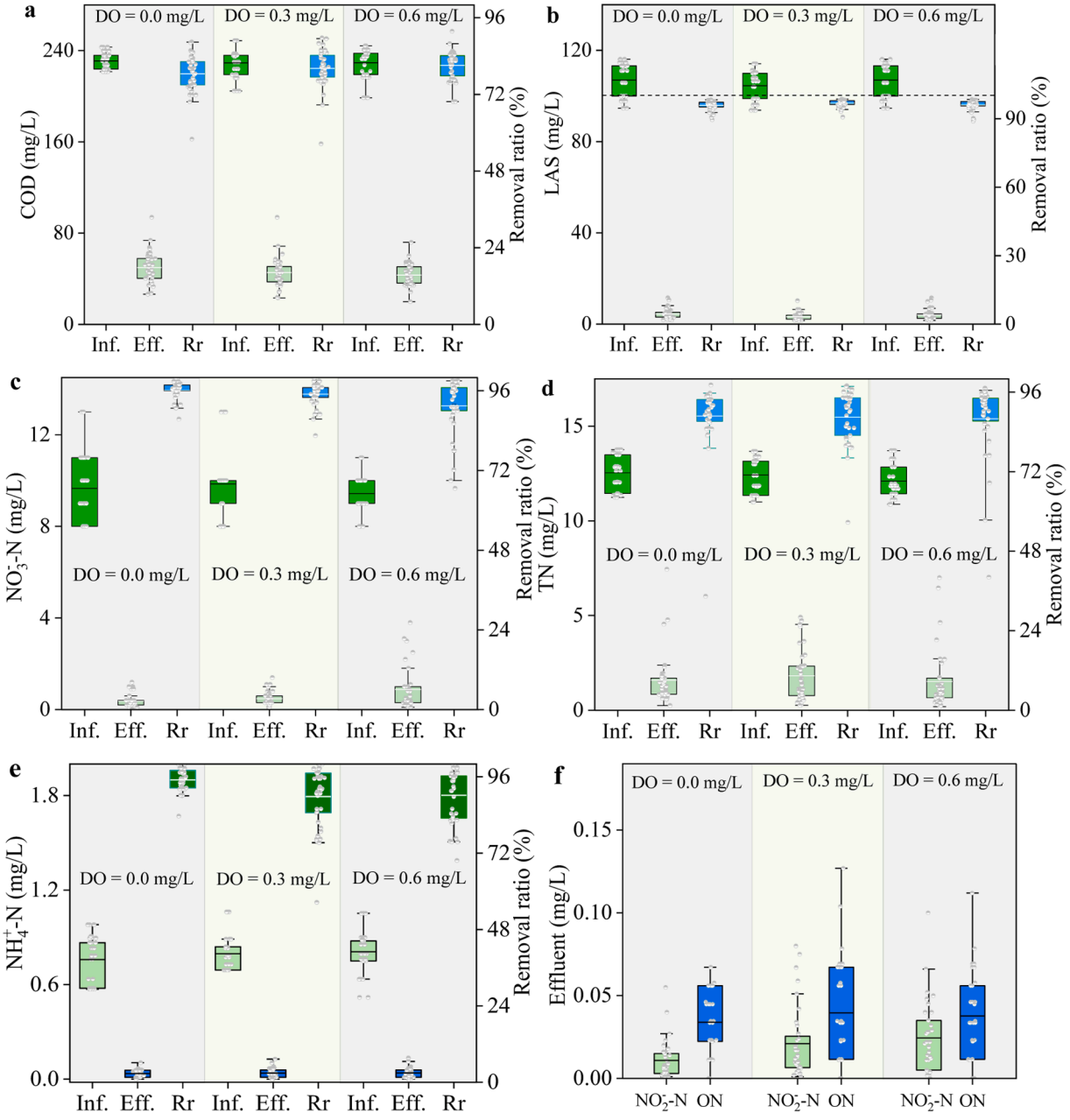

Fig. 1. Dynamics of concentrations and removal ratios of (a) COD, (b) LAS, (c) NO- 3-N, (d) TN and (e) NH+ 4-N, as well as the effluent concentrations of (f) NO- 2-N and organic nitrogen (ON) at various dissolved oxygen (DO) concentrations in the membrane aerated biofilm reactor (MABR) on day10–94 of operation.

2. Results

2.1. Reactor performance

Fig. 1 presents the removal of COD, LAS, NH+ 4-N, NO- 3-N, and TN, as well as the effluent NO- 2-N and organic nitrogen (ON) at different DO concentrations in the MABR; Fig. S1 shows the related long term operation plots. For organics removal, both COD and LAS showed similar effluent concentrations and removal efficiencies at three DO concentrations. DO at 0.6 mg/L achieved relatively better performance for LAS removal, consistent with previous findings that sufficient O_2 enabled complete LAS mineralization and 97 %−99 % of LAS can be removed in the aeration tank of wastewater treatment plant (Mungray and Kumar 2008). For N species, NH+ 4-N, NO- 3-N, and TN showed similar effluent concentrations and removal efficiencies at three DO conditions. DO at 0.0 mg/L achieved relatively better performance with low effluent NO-2-N and ON (Fig.S2). Notably, DO concentration in biofilm gradually dropped when increasing biofilm thickness until the lowest value in the bulk solution (Rittmann 2007). Lowest DO (0.0 mg/L) in the MABR enabled the formation of aerobic-anoxic-anaerobic multifunctional biofilm and achieved simultaneous and efficient removal of both organics and nitrogen (Zhou et al. 2020a; Zhou et al. 2020b).

2.2. Dynamics of effluent DOM molecular fractions

Fig. 2 shows the Van Krevelen diagram displaying H/C and O/C ratios, proportions and relative molecular weight of the component in effluent DOM. Lignin was the dominant components in DOM with the proportion of 83.6, 87.7 and 83.5 % at DO concentrations of 0.0, 0.3 and 0.6 mg/L, respectively. Lignin is the dominant fraction of DOM in the sediment and soil that can be derived from bacteria (Kellerman et al. 2018), which also showed low biodegradability and contributed to the main effluent components in biological wastewater treatment system (Li et al. 2018). Similarly, most of the ring activation-related intermediates (Table S1) during LAS removal in the MABR were located in region V representing lignin. Most of the degradation intermediates specific to aerobic environment landed in regions V (lignin) and VI (tannins), but which were found in regions II (proteins/amino sugars) and III (carbohydrates) under low DO conditions. Lignin- and tannins-like compounds are refractory organics, but the molecules in regions II and III are bioavailable organics due to higher H/C ratios and abundant hydrogenated structures (Osborne et al. 2013; Lusk and Toor 2016). This suggests that insufficient O_2 leads to inefficient biodegradation and accumulation of biodegradable organics. Consistent with previous findings that aromatic compound degrading microorganisms, they have a preference for non-sugar metabolites, such as non-aromatic organic acids or amino acids, rather than aromatic compounds; or for easily degradable aromatic compounds, such as benzoates, rather than more difficult substrates, such as toluene under anaerobic conditions (Wöhlbrand et al. 2007). LAS ($C_{18}H_{29}O_3S$, O/C = 0.16, H/C = 1.6) is located in region I ($0 < O/C \leq 0.3$, $1.5 < H/C \leq 2.0$), the proportions of effluent fractions belonging to this region in three DO conditions is also positively related to effluent LAS concentrations ($R^2 = 0.99$, $P < 0.01$) (Fig. S2). Most of the effluents DOM (>40 %) were accumulated at relative molecular weight (MW) of 300–350 with the highest proportion (60.9 %) at DO of 0.0 mg/L. For low MW fractions, high DO presented high relative abundance. This may be attributed by the fact that under high DO conditions, LAS undergoes alkyl chain breaking, benzene-ring cleavage and the MW of the intermediates is lower, while the anaerobic metabolic pathway produces intermediates containing coenzyme A structures resulting in less low MW fractions.

2.3. O_2-supply capacity significantly impacts microbial community structure

Fig. 3 presents the phylogenetic tree, predominant bacteria at phylum and genus levels, and the heatmap based differences in three reactors. The microbial community was dominated by Proteobacteria in the reactors with relatively high DO conditions (0.3 and 0.6 mg/L). The genera of *Denitratisoma, Limnobacter* and *Comamonadaceae* belonging to Proteobacteria are heterotrophic denitrifying bacteria, capable of oxidative metabolism of organic compounds using nitrate and nitrite as electron acceptor for respiration (Tian et al. 2021). Under low DO conditions (0.0 mg/L), the dominant taxa of Bacteroidetes is a common critical group in activated sludge that consist of gram-negative, non--spore-forming and rod-shaped bacteria (Gu et al. 2019). Bacteroidetes are key heterotrophs involved in cycling organic carbon and proteinaceous substances during anaerobic degradation process (Stevens et al. 2005). Other dominant taxa of hydrolytic acidifying bacteria, which belongs to Acidobacteria, are capable to degrade organics including saccharides (Feng et al. 2021). At genus level, the dominant groups at DO of 0.0 mg/L were *Limnobacter* and *Sulfuritalea*, which can grow autotrophically on hydrogen, thiosulfate and elemental sulfur, and heterotrophically on various organic substrates during denitrifying process (Watanabe et al. 2017). *Acidovorax* enables organics degradation in both nitrification and denitrification processes (Wu et al. 2022). *Flavobacterium, Denitratisoma* and *Hydrogenophaga*, playing key roles in heterotrophic denitrification process (Wang and Chu 2016), were prominent at DO concentrations of 0.3 and 0.6 mg/L.

For LAS removal (Fig. S3a), the typical aerobic degraders of *Hydrogenophaga, Parvibaculum, Pseudomonas* and *Flavobacterium* were relatively abundant at DO of 0.6 mg/L (Martínez-Pascual et al. 2010; Duarte et al. 2010). *Phenylobacterium*, a Gram-negative aerobic bacterium, plays a pivotal role in LAS degradation (Sánchez-Peinado Mdel et al. 2010), and showed high abundance at all conditions in the MABR. its relative abundance peaked at 2.327 % at DO = 0.3 mg/L and reached 1.670 % at DO = 0.0 mg/L. This may account for the aerobic-anaerobic-anoxic multifunctional biofilm formed in the DO = 0.0 mg/L reactor (Zhou et al., 2020a), which simultaneously performs aerobic and anaerobic metabolism to achieve efficient reduction of LAS and nitrogen. Under anaerobic conditions, *Desulfovibrio, Desulfomicrobium, Desulfomonile* and *Desulfonema* can degrade aromatic compounds and enabled the efficient removal of LAS (Duarte et al. 2010; Okada et al. 2014), *Geobacter* was reported to degrade aromatic contaminants by oxidative ring cleavage under strictly anaerobic conditions (Schleinitz et al. 2009).

For nitrogen metabolism (Fig. S3b), *Pseudomonas* is a relatively common genus of heterotrophic aerobic denitrifying bacteria, which has high capability to remove ammonia nitrogen, nitrate and nitrite through heterotrophic denitrification, and grows much faster in the environment than autotrophic genera (He et al. 2016; Wang et al. 2018). As a heterotrophic genus of facultative denitrifying bacteria, *Arenimonas* has relatively high abundance in DO = 0.6 mg/L, which can absorb and utilize organic carbon sources. Studies mention it is involved in the degradation of complex and difficult to degrade organic compounds such as penicillin, carbamazepine and bisphenol A (Huang et al. 2021; Rutere et al. 2020). *Flavobacterium* is also an aerobic denitrifying bacterium and *Denitratisoma* is a genus of filamentous denitrifying bacteria commonly found in anaerobic reactors (Su et al. 2022). *Acidovorax* was regarded as a nitrate-dependent iron-oxidizing bacteria (Bai et al. 2023). Efficient removal of LAS at three DO conditions are contributed to the coexistence and synergistic interaction of multiple functional bacteria in the multifunction biofilm, but different O_2 supply capacities showed specific dominant bacterial groups and predominant metabolic pathways.

3. Discussion

Aerobic condition with higher-than-demand O_2 supply can achieve complete LAS mineralization (Pakou et al. 2007) and C atoms less than five enabled desulfonation and ring cleavage as microbes favor arylsulphonate rather than alkylbenzene sulphonate (Cain 1987). Desulfonation involves the introduction of two O atoms into the substrate

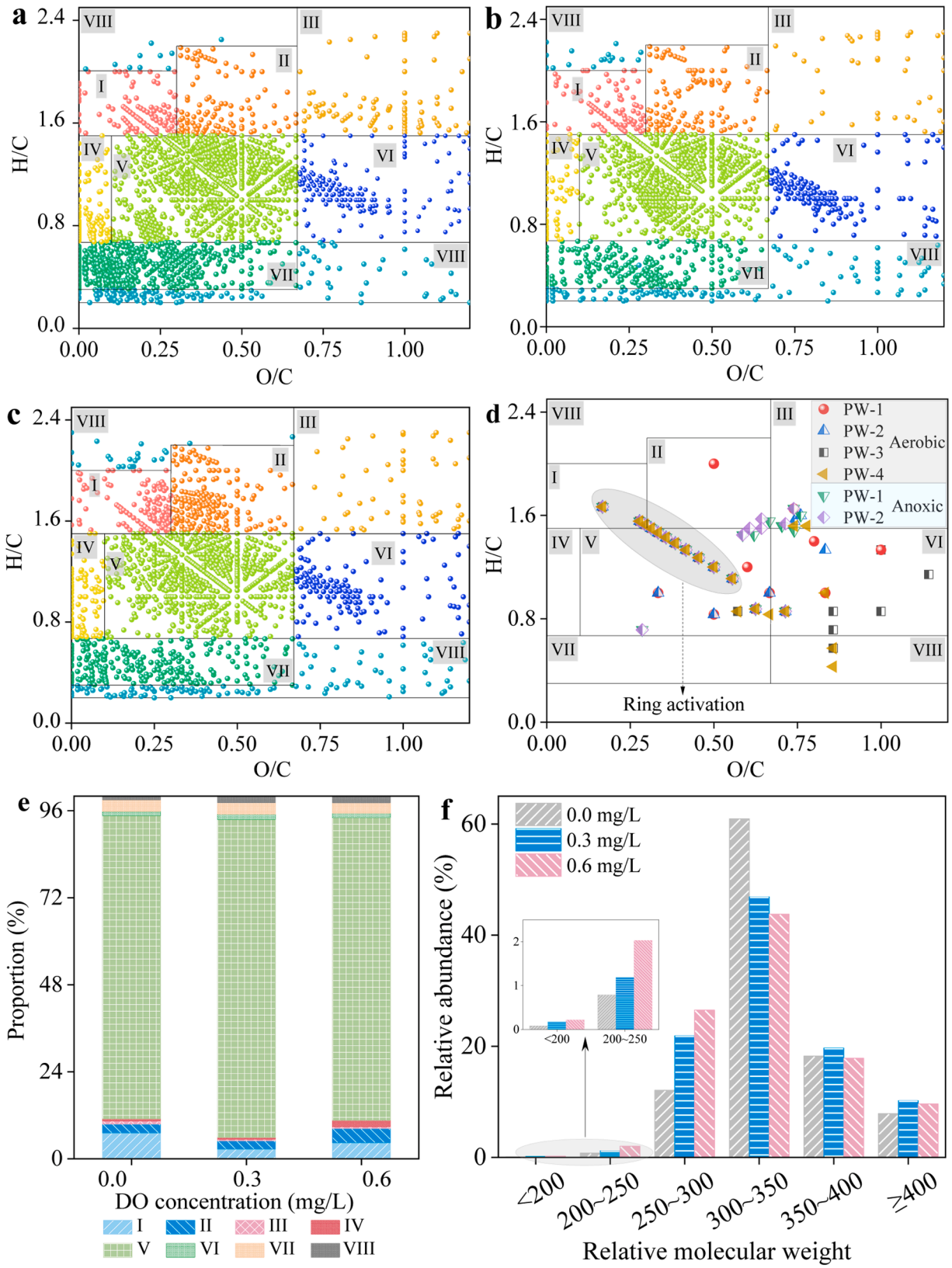

Fig. 2. Van Krevelen diagrams compare dissolved organic matters (DOM) at dissolved oxygen (DO) concentrations of (a) 0.0 mg/L, (b) 0.3 mg/L, (c) 0.6 mg/L, and (d) the information of intermediate products at the noted LAS metabolic pathways at high and low DO concentrations; (e) the related proportions of molecules at the noted region and (f) the relative abundance of molecular weight at the noted DO condition in the membrane aerated biofilm reactor. Molecules in the diagrams contain (I) lipids, (II) proteins/amino sugars, (III) carbohydrates, (IV) unsaturated hydrocarbons, (V) lignin, (VI) tannins, (VII) condensed aromatics and (VIII) other components.

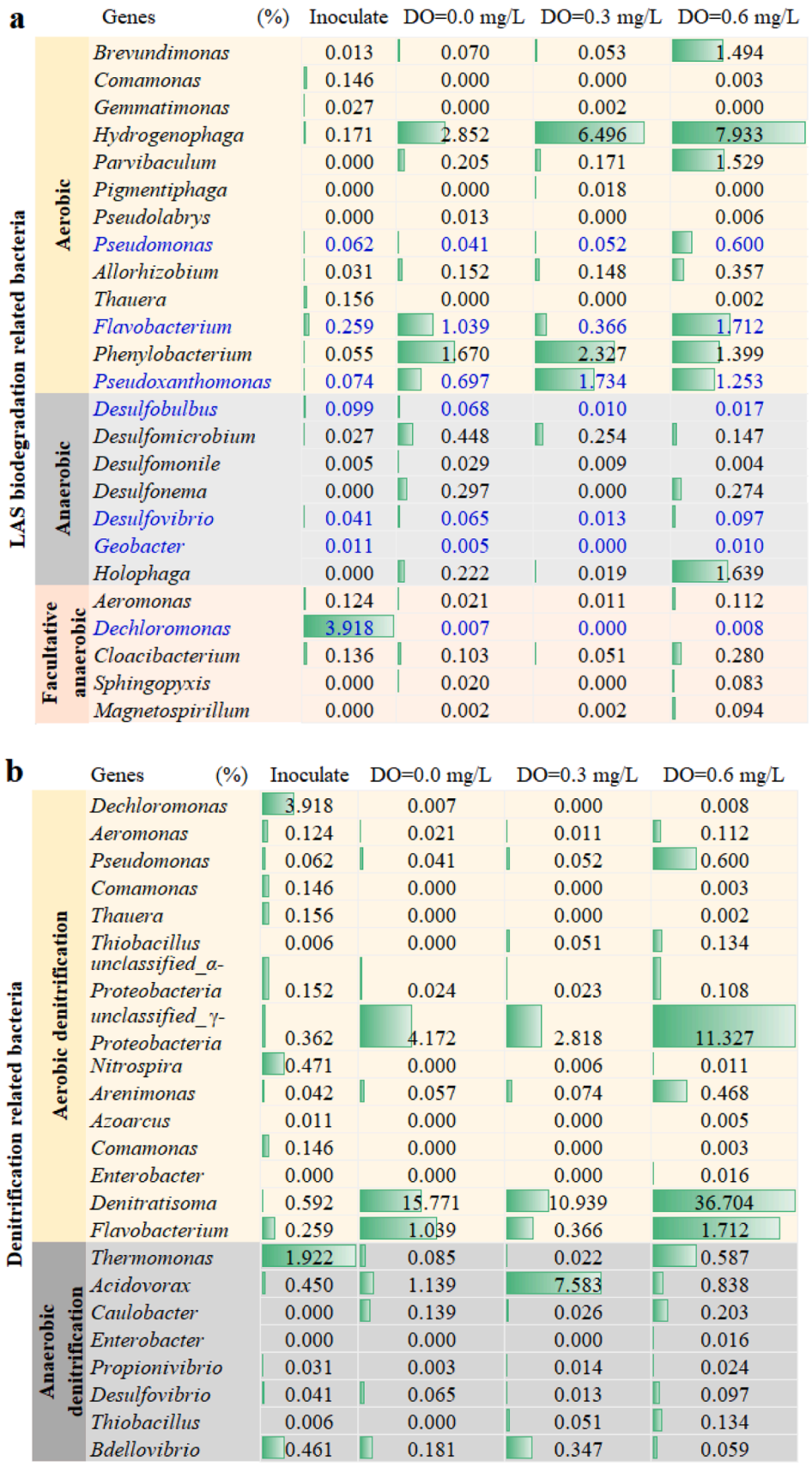

Fig. 3. Dynamics of the relative abundances of biofilm microbial communities functional for (a) linear alkylbenzene sulfonate (LAS) biodegradation and (b) denitrification at genus level under various dissolved oxygen concentrations in the membrane aerated biofilm reactor. The text in blue represents the genera that can metabolize LAS with nitrate as electron acceptor.

molecule through a complex enzyme system including 4-sulfobenzoate 3,4-dioxygenase (EC1.14.12.8), which also activates the stable benzene ring (Locher et al. 1991). Fig. 4 shows the metabolic pathways and related functional enzymes of LAS, and denitrification related enzymes at the noted DO concentration and Fig. 5 presents the possible metabolic pathways at different O_2 supply conditions. Table S2 shows the in detail information of related enzymes and catalyzed reactor of LAS in different metabolic pathways and Fig. S4 shows the detection of LAS and three key intermediate products during biological LAS mineralization. In MABR with sufficient O_2 supply, four possible benzene ring cleavage pathways were detected including catechol ortho-cleavage (EC1.13.11.1), catechol meta-cleavage (EC1.13.11.2), 3,4-dihydroxybenzoate (aka protocatechuic acid, PCA) meta-cleavage (EC 1.13.11.8) and PCA ortho-cleavage (EC1.13.11.3), all of which showed the relatively higher abundance at DO concentration of 0.3 and 0.6 mg/L. Significant abundance of functional enzymes encoding the whole aerobic pathways 1, 2 and 4 in MABR suggested that microorganisms in biofilm achieved LAS mineralization mainly through catechol ortho-cleavage, catechol meta-cleavage and PCA ortho-cleavage. Relatively high abundance of enzymes functional for PCA meta-cleavage (pathway 3) at high DO conditions ($\geq$ 0.3 mg/L) indicated that sufficient O_2 supply showed a larger microbial community and enabled efficient LAS biodegradation through multiple aerobic metabolic pathways. In addition, high abundance of functional enzymes in aerobic denitrifiers including nitrate reductase, nitronate monooxygenase, nitrite reductase (NO forming and NADH) and nitric-oxide reductase in aerobic conditions further suggested that aerobic oxidation combined with aerobic denitrification-coupled utilization achieved complete LAS mineralization with higher-than-demand O_2 supply.

It has been shown that under insufficient or fluctuating O_2 conditions, LAS was converted to benzoic acid or phenylacetic acid after ω- and β-oxidation and desulfonation of the alkyl side chain (Fuchs et al. 2011). In the MABR, two possible anaerobic metabolic pathways of LAS existed according to the metagenomic detected functional enzymes, which showed relatively high abundance at low O_2 supply capacity (0.0 mg/L that only account for 27.4 % of O_2 demand for complete LAS mineralization). Phenylacetic acid can be catalyzed to phenylacetyl-CoA by AMP-forming benzoate-CoA ligase (EC 6.2.1.25) and ATP that exist in *Colletotrichum, Lenzites, Rhodovulum Streptomyces* and other genera. Phenylacetyl-CoA monooxygenase (EC 1.14.13.149) can achieve the sub-sequent conversion of phenylacetyl-CoA to non-aromatic ring 1, 2-epoxyphenyl-acetyl-CoA with supplied O_2 (Grishin et al. 2011). If O_2 is not accessible, phenylacetyl-CoA will be catalytic dearomatized by cyclohexa-1,5-diene-1-carbonyl -CoA (EC 1.3.7.8), achieving the destability of benzene ring. Under insufficient O_2 conditions, alkyl side chains oxidization and dearomatization requires a small amount of O_2, which relies on the anaerobic respiration process using alternative electron acceptors (nitrate, sulfate, Fe^{3+}) (Gottschalk 1986), which also explained that nitrate respiration improved denitrification-coupled LAS biodegradation in the MABR at restricted O_2 conditions. Moreover, high abundance of functional enzymes in both aerobic and anaerobic denitrifies including hydroxylamine reductase, nitrous-oxide reductase and nitrite reductase (cytochrome, ammonia forming) in anaerobic conditions further suggested that aerobic activation and anaerobic denitrification- coupled utilization enabled efficient LAS biodegradation at restricted O_2 conditions.

Efficient and low-energy-input LAS removal is essential for safe discharge and potential reuse of wastewater. In the MABR, hollow-fiber membrane supplies O_2 accurately at bubble-free diffusion mode and enables the attachment of microbes for biofilm formation (Lai et al. 2017; Martin and Nerenberg 2012), which achieved efficient removal of LAS at both sufficient and insufficient O_2 supply conditions (Fig. 6). With higher-than-demand O_2 supply (DO = 0.6 mg/L), MABR achieved efficient removal through full mineralization (predominant) and aerobic denitrification-coupled biodegradation by multiple related microbes and functional enzymes with four possible LAS aerobic metabolic pathways. As O_2 dosage was reduced to only 29.7 % of the demand for full LAS mineralization, part of O_2 respiration was replaced by NO- 3-N respiration. In this stage, O_2 was functional for LAS activation, benzene-ring cleavage and aerobic respiration, but NO- 3-N respiration related anaerobic denitrification also contributed to ring-opening organics' removal. Combined with four aerobic metabolic pathways, *Desulfomicrobium* and *Desulfonema* related to two possible anaerobic metabolic pathways enabled efficient removal of LAS. Elucidation of microaerobic activated co-metabolism of LAS and nitrate at low DO conditions is important to further reduce the treatment cost of industrial wastewater from LAS production and source-diverted greywater, which provides a promising alternative strategy for reducing energy and economic costs in LAS full mineralization (Shaikh et al. 2019), and favors the practical application of MABR in wastewater treatment. Future work should be focused on achieving efficient LAS mineralization in anaerobic systems to further reduce wastewater treatment cost, which should depend on selecting the suitable alternative electron acceptors including sulphate, hydrogen sulfide, carbonate yield, methane and ammonia (Mungray and Kumar 2009).

4. Conclusion

MABR enabled efficient removal of organics and nitrogen at different DO concentrations. Adequate O_2 supply facilitated LAS removal through mineralization (predominant) and aerobic denitrification-coupled biodegradation with four possible LAS aerobic metabolic pathways. As O_2 dosage reduced to only 29.7 % of the demand for full LAS mineralization, part of O_2 respiration was replaced by NO- 3-N respiration. O_2 was functional for LAS activation, benzene-ring cleavage and aerobic respiration, but NO- 3-N respiration related anaerobic denitrification also contributed to ring-opening organics' removal. Combined with four aerobic metabolic pathways, *Desulfomicrobium* and *Desulfonema* related two possible anaerobic metabolic pathways enabled efficient removal of LAS. Low O_2-supply coupled anaerobic respiration dependent MABR provides a promising alternative strategy for reducing energy and economic costs in complete LAS mineralization.

5. Methods and materials

5.1. Setup, inoculation and continuous operation of MABR

The MABR system consisted of an acrylic cylinder, rubber hoses, two peristaltic pumps (BT100–2 J, Longer Pump®, China) for providing influent and completely mixing (Fig. S5). The reactor contained eight bundles of polyvinylidene fluoride (PVDF) hollow fibers (length of 28 cm and outside diameter of 1.2 mm) with the average pore size lower than 0.02 μm, which provides continuous bubbleless O_2 supply for biofilm growth (Zhou et al. 2020a). Three MABRs were used for the study. By adjusting lumen air pressure every day through a controllable air pump (SB-948, SEBO, China), DO concentrations in three MABRs were maintained at 0.0, 0.3 and 0.6 mg/L, respectively.

The synthetic LAS-containing medium was prepared in a 10-L bottle and O_2 in the medium was removed by blowing pure nitrogen gas for 10 min. The feeding medium were consisted of (in mg/L) 1.125 KH_2PO_4, 1.125 K_2HPO_4, 1.029 $CaCl_2{\cdot}2H_2O$, 1.998 $MgCl_2$, 0.493 $MgSO_4{\cdot}7H_2O$, 0.398 $FeCl_2{\cdot}4H_2O$, 336 $NaHCO_3$, 100 dodecyl benzene sulfonate (DBS, 348.48 g mol^{-1}), 10.5 $NaNO_3$, 0.8 NH_4Cl and 1mL/L trace element solution (Chung et al. 2006; Liu et al. 2018b). Carbon source in the medium is only contributed from LAS, which was purchased Shanghai Chem. Co. Ltd., China. The inoculum activated sludge was obtained from the secondary sedimentation tank of Tangxun Lake wastewater treatment plant (Wuhan, China) with the biomass concentration of 1.50 ± 0.19 g TSS/L. The MABRs were initially operated in batch mode for one day to allow the biomass to form on the surface of membrane fibers (Zhou et al. 2020a), with the conditions of 10-mL of feeding medium, room temperature at 21.7 ± 1.2 °C and internal circulation time of 2

a

	Pathway	EC	Enzyme	Inoclum	0.0 mg/L	0.3 mg/L	0.6 mg/L
Aerobic condition	PW-1	1.13.11.2	Catechol 2,3-dioxygenase	0.186	0.104	0.181	0.173
		1.1.1.95	Phosphoglycerate dehydrogenase	1.990	1.817	2.042	1.691
		4.1.1.77	2-oxo-3-hexenedioate decarboxylase	0.055	0.106	0.181	0.231
		4.2.1.80	2-oxopent-4-enoate hydratase	0.120	0.091	0.130	0.170
		4.1.3.39	4-hydroxy-2-oxovalerate aldolase	0.125	0.147	0.190	0.167
		1.2.1.3	Aldehyde dehydrogenase (NAD(+))	1.663	1.586	1.929	1.565
		6.2.1.1	Acetate--CoA ligase	1.599	1.888	1.799	2.082
	PW-2	1.13.11.1	Catechol 1,2-dioxygenase	0.023	0.011	0.025	0.023
		5.5.1.1	Muconate cycloisomerase	0.018	0.005	0.013	0.018
		3.1.1.45	Carboxymethylenebutenolidase	1.255	1.333	1.863	1.536
		5.3.3.4	Muconolactone Delta-isomerase	0.039	0.092	0.088	0.040
		3.1.1.24	3-oxoadipate enol-lactonase	0.193	0.236	0.307	0.206
		2.8.3.6	3-oxoadipate CoA-transferase	0.177	0.272	0.524	0.143
		2.3.1.16	Acetyl-CoA C-acyltransferase	1.174	1.018	1.183	1.136
		2.3.1.9	Acetyl-CoA C-acetyltransferase	3.700	3.944	4.532	4.328
	PW-3	1.13.11.8	Protocatechuate 4,5-dioxygenase	0.145	0.200	0.476	0.469
		1.1.1.312	2-hydroxy-4-carboxymuconate semialdehyde hemiacetal dehydrogenase	0.059	0.073	0.237	0.134
		3.1.1.57	2-pyrone-4,6-dicarboxylate lactonase	0.066	0.074	0.240	0.137
		5.3.2.8	4-oxalomesaconate tautomerase	0.005	0.006	0.011	0.013
		4.2.1.83	4-oxalmesaconate hydratase	0.081	0.080	0.254	0.154
		4.1.3.17	4-hydroxy-4-methyl-2-oxoglutarate aldolase	0.098	0.082	0.257	0.153
	PW-4	1.13.11.3	Protocatechuate 3,4-dioxygenase	0.119	0.166	0.243	0.181
		5.5.1.2	3-carboxy-cis,cis-muconate cycloisomerase	0.077	0.068	0.067	0.028
		4.1.1.44	4-carboxymuconolactone decarboxylase	0.501	0.590	0.897	0.509
		3.1.1.24	3-oxoadipate enol-lactonase	0.193	0.236	0.307	0.206
		2.8.3.6	3-oxoadipate CoA-transferase	0.177	0.272	0.524	0.143
		2.3.1.9	Acetyl-CoA C-acetyltransferase	3.700	3.944	4.532	4.328
		2.3.1.16	Acetyl-CoA C-acyltransferase	1.174	1.018	1.183	1.136
		6.2.1.5	Succinate--CoA ligase (ADP-forming)	2.552	2.652	2.407	2.471
Anoxic condition	PW-1	1.2.1.10	Acetaldehyde dehydrogenase (acetylating)	0.172	0.184	0.223	0.173
		6.2.1.25	Benzoate--CoA ligase	0.060	0.126	0.284	0.127
		1.14.13.149	Phenylacetyl-CoA 1,2-epoxidase	0.466	0.675	0.727	1.198
		4.1.2.44	Benzoyl-CoA-dihydrodiol lyase	0.106	0.113	0.216	0.119
		1.2.1.4	Aldehyde dehydrogenase (NADP(+))	0.128	0.130	0.208	0.156
		2.3.1.174	3-oxoadipyl-CoA thiolase	0.019	0.034	0.042	0.031
	PW-2	1.3.7.8	Benzoyl-CoA reductase	0.002	0.000	0.000	0.002
		4.2.1.100	Cyclohexa-1,5-dienecarbonyl-CoA hydratase	0.000	0.000	0.000	0.001
		1.1.1.35	3-hydroxyacyl-CoA dehydrogenase	1.645	1.772	2.149	2.296
		1.3.8.7	Medium-chain acyl-CoA dehydrogenase	1.752	1.925	2.698	2.218
		4.2.1.17	Enoyl-CoA hydratase	2.609	2.851	3.239	3.175

b

	EC	Enzyme	(‰) Inoclum	0.0 mg/L	0.3 mg/L	0.6 mg/L
Denitrification	1.7.7.2	Ferredoxin--nitrate reductase	0.051	0.033	0.042	0.019
	1.7.99.4	Nitrate reductase	1.231	1.884	2.014	2.413
	1.13.12.16	Nitronate monooxygenase	1.017	1.518	1.728	2.049
	1.7.2.1	Nitrite reductase (NO-forming)	0.249	0.489	0.387	0.561
	1.7.99.1	Hydroxylamine reductase	0.227	0.376	0.136	0.224
	1.7.1.15	Nitrite reductase (NADH)	1.143	1.458	1.712	1.984
	1.7.2.4	Nitrous-oxide reductase	0.236	0.113	0.083	0.057
	1.7.2.5	Nitric-oxide reductase (cytochrome c)	0.264	0.171	0.247	0.379
	1.7.2.2	Nitrite reductase (cytochrome; ammonia-forming)	0.042	0.228	0.094	0.031

Fig. 4. Dynamics of related enzyme abundance functional for in the inoculum and biofilm samples at various dissolved oxygen concentrations conditions at (a) various linear alkylbenzene sulfonate (LAS) metabolic pathways and (b) denitrification process under high and low dissolved oxygen concentrations in the membrane aerated biofilm reactor according to biofilm metagenomic data.

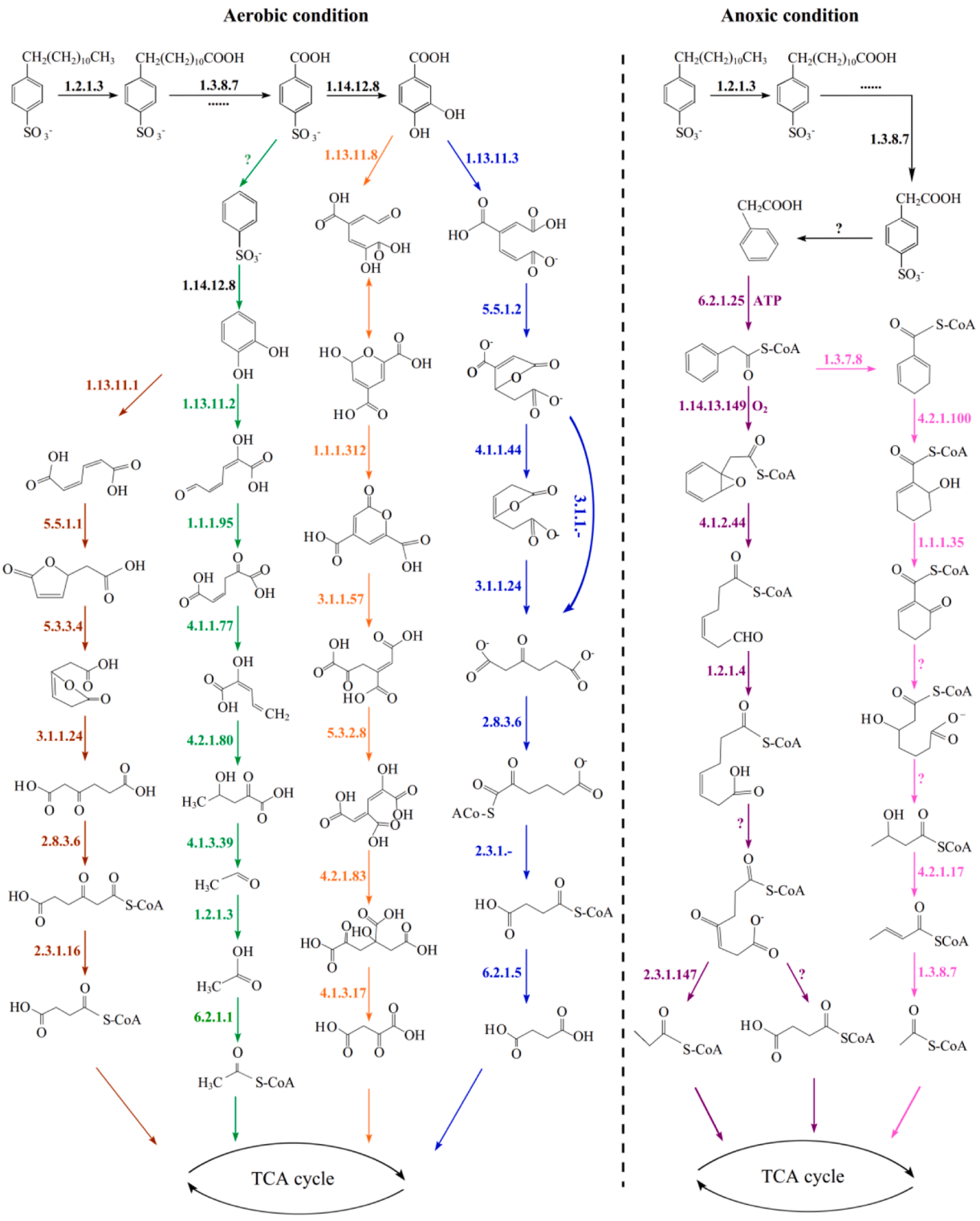

Fig. 5. Reconstruction of possible metabolic pathways of linear alkylbenzene sulfonate (LAS) oxidation toward tricarboxylic acid (TCA) cycle based on the KEGG database and the metagenomic results on potential abundances of genes encoding all the enzymes responsible for each of the four parallel yet distinct aerobic and two anoxic metabolic pathways in the membrane aerated biofilm. Each colored arrow portraits an enzyme involved in the metabolism with an Enzyme Commission (EC) number as assigned by KEGG database. Names and catalyzed pathways of the enzymes with EC numbers are listed in Table S2.

min. Then, the MABRs were continuously operated for 94 days with the same hydraulic retention time of 12 h, and all MABRs can reach the steady state after operated for 10 days. The detailed information of continuously operated MABRs is shown in Table S3.

5.2. Sample collection and analytical methods

Liquid samples were collected from the MABRs every two days and stored in 50-mL polypropylene centrifuge tubes at 4 °C. The stored samples were initially filtered by 0.22-μm filter (JinTeng, China) and then used for the analyses of LAS and nitrogen removal and effluent

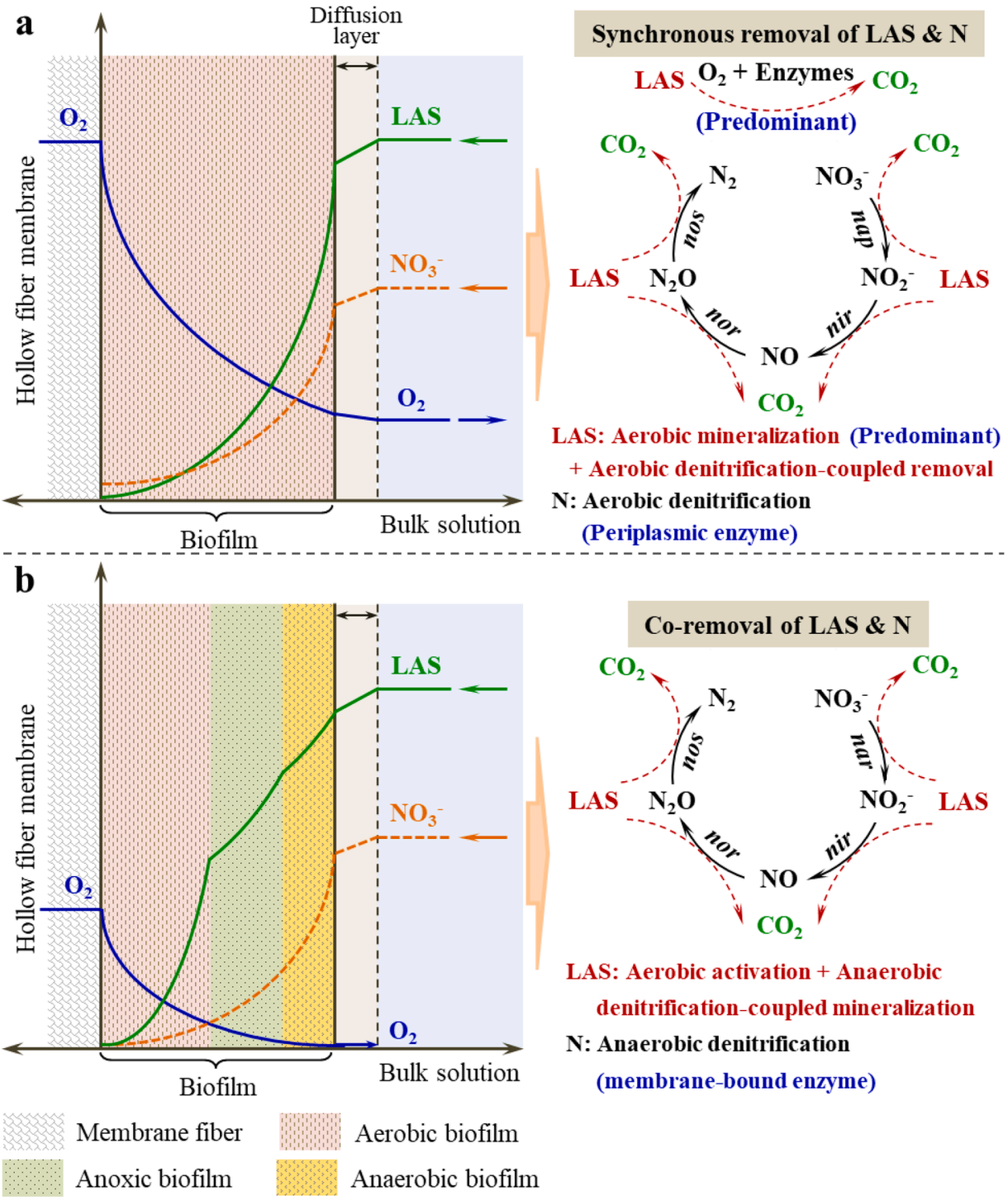

Fig. 6. Proposed gradient profiles of oxygen (O_2), linear alkylbenzene sulfonate (LAS) and nitrate concentrations (left panel), as well as the related LAS and nitrogen metabolic pathway (right panel) in the bubble-free air-supply biofilm with high (a) and low (b) dissolved oxygen condition.

DOM characteristics. At the end of the operation, 5 mL homogenized biofilm samples were collected from each MABR and stored at −20 °C for genomic DNA extraction.

The concentrations of COD, TN and NH+ 4-N were determined using standard methods (APHA 2017). NO- 3-N and NO- 2-N concentrations were measured using a benchtop spectrophotometer (DR 3900, HACH, USA) with nitrate and nitrite kits (HACH®, USA) with the test limitation of 30 mg/L and 0.5 mg/L, respectively. Organic N (ON) was equal to TN minus inorganic N including NH+ 4-N, NO- 3-N and NO- 2-N. LAS concentration was determined using the methylene blue spectrophotometric method (Zhou et al. 2019; Zhou et al. 2020a). DO concentration in the bulk liquid of MABR was monitored using a portable DO meter (Rex DO-957-Q, Rex Electric Chemical, Shanghai, China). Lumen air pressure inside the membrane module was determined using a portable pressure meter (GMH 3100 Greisinger, Germany). The intermediate products of LAS mineralization were identified using liquid chromatography coupled with tandem mass spectroscopy (LC-MS/MS), and the detailed information was shown in Table S4 and the Supporting Information. The distribution, proportion and molecular weight of the fractions in the effluent DOM were analyzed using Fourier

transform ion cyclotron resonance mass spectrometry (FTICR-MS, Bruker SolariX, Bruker, Germany) equipped with an electrospray ionization (ESI) source. The known series CHO-like compounds in DOM were used to internally recalibrate the spectra with the quality errors lower than 1 ppm. Molecular formula of the main components in DOM was obtained according to the H/C and O/C ratios (Lin et al. 2021), and visualization of the obtained data was achieved using the van Krevelen diagram (Laszakovits and MacKay 2022). The detailed procedures and data analysis methods are available in Section1.1 of the SI.

5.3. Calculation of O_2-supply dosage

For the complete mineralization of LAS under aerobic conditions, the maximum O_2 demand ($J_{O2,\ max}$) was calculated according to following equation:

$$J_{O2,\ max} = 2.25 q_{LAS} \quad (1)$$

Where q_{LAS} (mg LAS/h) is the influent flow rate of LAS in the MABR, 2.25 (g O_2/g LAS) is the O_2 equivalent to achieving full LAS mineralization (Zhou et al. 2020b). With the influent flow rate and LAS concentration at 7.2 mL/min and 100 mg/L, respectively, the value of $J_{O2,\ max}$ should be 9.72 mg O_2/h. According to our previous findings that the PVDF hollow fibers can achieve an O_2-supply rate (OSR) of 86.6 mg O_2/(m^2·h·psi) at room temperature (21.5 ± 0.3 °C) (Zhou et al. 2020a). O_2-supply capacity of the MABR can be obtained according to following equation:

$$J_{O2} = OSR \cdot LAP \cdot S \quad (2)$$

where LAP (psi) is the lumen air pressure of membrane fibers and S (m^2) is the total surface area of the membrane module. Thus, with the lowest DO (0.00 mg/L, LAP = 0.094 psi) in the MABR (Table S3), O_2-supply capacity was only 29.7 % of the demand for complete LAS mineralization.

5.4. Biofilm DNA extraction and metagenomic analysis

The microbial analysis methods used in this study are all based on gene presence rather than expression. Genomic DNA extraction of inoculated biofilm samples and biofilm samples after reactor operation were achieved using a SPINeasy DNA Kit for soil (MP Biomedicals, California, USA) according to the manufacturer's protocol. DNA purification and quantification were achieved in a NanoDrop One/OneC (Thermo Scientific, US). DNA samples were stored at −70 °C until following processing and analyzing. The DNA samples were sent to Shanghai Personalbio technology Co., Ltd (Shanghai, China) for metagenomic sequencing in NovaSeq platform (Illumina) with a paired-end (2 × 100) sequencing strategy. The Personal Gene Cloud and online software QIIME2 were used to microbial community analysis (https://view.qiime2.org/). Customized data processing pipeline was performed to retrieve metagenome-assembled genomes (MAGs). Taxonomic classification, including all available bacterial and algal genomes, was achieved by Kraken2 (v2.0.12) against the NCBI RefSeq database (Wood et al. 2019). EnrichM (version 0.5.0) was applied for the identification of Kyoto Encyclopedia of Genes and Genomes (KEGG) functional orthologs (i.e., EC) in each MAG (Lin et al. 2021). Normalizing reads per million reads was used for indicating the relative abundance of functional genes.

5.5. Statistical analysis

The OriginPro 2020 software (OriginLab Corp, Northampton, USA) was used to analyze the raw data of reactor performance. TSS, DO, COD, LAS, NH+ 4-N, NO- 3-N, NO- 2-N, TN, LAP were measured in triplicate for each sample, and results were expressed as the mean and standard deviation (mean ± SD). Three soluble liquid samples at the noted sampling time in each MABR were well-mixed for one-time FTICR-MS characterization. Microbial abundance was visualized and downloaded on the online QIIME2, then further analyzed by Excel 2021 screening (Microsoft Corp, Washington, USA) and OriginPro 2020 software. The possible metabolic pathways of LAS oxidation toward tricarboxylic acid (TCA) cycle were plotted on InDraw software (Integle Information Technology Co., LTD, Shanghai, China).

CRediT authorship contribution statement

Ting Wei: Writing – original draft, Visualization, Software, Methodology, Investigation, Formal analysis, Data curation. **Ting Ran:** Writing – review & editing, Visualization, Software. **Weikang Rong:** Writing – review & editing, Visualization, Software, Data curation. **Yun Zhou:** Writing – review & editing, Supervision, Project administration, Funding acquisition, Conceptualization.

Declaration of competing interest

The authors declare that they have no known competing financial interests or personal relationships that could have appeared to influence the work reported in this paper.

Acknowledgements

This research was supported by National Natural Science Foundation of China (52200054), the Fundamental Research Funds for the Central Universities (303-510324066) and the Startup Funding for Returned Scholars in Huazhong Agricultural University (303-11042010013).

Supplementary materials

Supplementary material associated with this article can be found, in the online version, at doi:10.1016/j.wroa.2024.100268.

Data availability

Data will be made available on request.

References

Angelidaki, I., Mogensen, A.S., Ahring, B.K., 2000. Degradation of organic contaminants found in organic waste. Biodegradation 11 (6), 377–383.
APHA, 2017. Standard Methods For the Examination of Water and Wastewater, 20th ed. American Public Health Association, Washington, DC, New York.
Babaei, F., Ehrampoush, M.H., Eslami, H., Ghaneian, M.T., Fallahzadeh, H., Talebi, P., Fard, R.F., Ebrahimi, A.A., 2019. Removal of linear alkylbenzene sulfonate and turbidity from greywater by a hybrid multi-layer slow sand filter microfiltration ultrafiltration system. J. Clean. Prod. 211, 922–931.
Bai, Y., Wang, S., Zhussupbekova, A., Shvets, I.V., Lee, P.-H., Zhan, X., 2023. High-rate iron sulfide and sulfur-coupled autotrophic denitrification system: nutrients removal performance and microbial characterization. Water Res. 231, 119619.
Cain, R.B., 1987. Biodegradation of anionic surfactants. Biochem. Soc. Trans. 15 (Suppl), 7s–22s.
Chung, J., Nerenberg, R., Rittmann, B.E., 2006. Bioreduction of selenate using a hydrogen-based membrane biofilm reactor. Environ. Sci. Technol. 40 (5), 1664–1671.
Denger, K., Cook, A.M., 1999. Linear alkylbenzenesulphonate (LAS) bioavailable to anaerobic bacteria as a source of sulphur. J. Appl. Microbiol. 86 (1), 165–168.
Duarte, I.C.S., Oliveira, L.L., Mayor, M.S., Okada, D.Y., Varesche, M.B.A., 2010. Degradation of detergent (linear alkylbenzene sulfonate) in an anaerobic stirred sequencing-batch reactor containing granular biomass. Int. Biodeterior. Biodegradation 64 (2), 129–134.
Elsgaard, L., 2010. Toxicity of xenobiotics during sulfate, iron, and nitrate reduction in primary sewage sludge suspensions. Chemosphere 79 (10), 1003–1009.
Feng, L., Song, J., Gu, H., Zhen, X., 2021. Mechanism of contaminant removal by algae-bacteria symbiosis in a PBR system during the treatment of anaerobic digestion effluents. Agric. Water Manag. 247, 106556.
Fuchs, G., Boll, M., Heider, J., 2011. Microbial degradation of aromatic compounds - from one strategy to four. Nat. Rev. Microbiol. 9 (11), 803–816.
Garcia, M.T., Campos, E., Ribosa, I., Latorre, A., Sánchez-Leal, J., 2005. Anaerobic digestion of linear alkyl benzene sulfonates: biodegradation kinetics and metabolite analysis. Chemosphere 60 (11), 1636–1643.

Gejlsbjerg, B., Andersen, T.T., Madsen, T., 2004. Mineralization of organic contaminants under aerobic and anaerobic conditions in sludge-soil mixtures. J. Soils Sediments 4 (1), 30–36.
Gottschalk, G., 1986. Bacterial Metabolism. Springer, New York, NY, New York.
Grishin, A.M., Ajamian, E., Tao, L., Zhang, L., Menard, R., Cygler, M., 2011. Structural and Functional Studies of the Escherichia coli Phenylacetyl-CoA Monooxygenase Complex*. J. Biol. Chem. 286 (12), 10735–10743.
Gu, Y., Wei, Y., Xiang, Q., Zhao, K., Yu, X., Zhang, X., Li, C., Chen, Q., Xiao, H., Zhang, X., 2019. C:n ratio shaped both taxonomic and functional structure of microbial communities in livestock and poultry breeding wastewater treatment reactor. Sci. Total. Environ. 651 (Pt 1), 625–633.
He, T., Li, Z., Sun, Q., Xu, Y., Ye, Q., 2016. Heterotrophic nitrification and aerobic denitrification by Pseudomonas tolaasii Y-11 without nitrite accumulation during nitrogen conversion. Bioresour. Technol. 200, 493–499.
Huang, S., Yu, D., Chen, G., Wang, Y., Tang, P., Liu, C., Tian, Y., Zhang, M., 2021. Realization of nitrite accumulation in a sulfide-driven autotrophic denitrification process: simultaneous nitrate and sulfur removal. Chemosphere 278, 130413.
Jensen, J., 1999. Fate and effects of linear alkylbenzene sulphonates (LAS) in the terrestrial environment. Sci. Total Environ. 226 (2), 93–111.
Kellerman, A.M., Guillemette, F., Podgorski, D.C., Aiken, G.R., Butler, K.D., Spencer, R.G. M., 2018. Unifying Concepts Linking Dissolved Organic Matter Composition to Persistence in Aquatic Ecosystems. Environ. Sci. Technol. 52 (5), 2538–2548.
Kim, N.-K., Lee, S.-H., Yoon, H., Jeong, G., Jung, Y.-J., Hur, M., Lee, B.-H., Park, H.-D., 2021. Microbiome degrading linear alkylbenzene sulfonate in activated sludge. J. Hazard. Mater. 418, 126365.
Lai, Y.S., Ontiveros-Valencia, A., Ilhan, Z.E., Zhou, Y., Miranda, E., Maldonado, J., Krajmalnik-Brown, R., Rittmann, B.E., 2017. Enhancing biodegradation of C16-alkyl quaternary ammonium compounds using an oxygen-based membrane biofilm reactor. Water Res. 123, 825–833.
Lara-Martín, P.A., Gómez-Parra, A., Köchling, T.K., Sanz, J.L., Amils, R., González-Mazo, E., 2007. Anaerobic degradation of linear alkylbenzene sulfonates in coastal marine sediments. Environ. Sci. Technol. 41 (10), 3573–3579.
Laszakovits, J.R., MacKay, A.A., 2022. Data-Based Chemical Class Regions for Van Krevelen Diagrams. J. Am. Soc. Mass Spectrom. 33 (1), 198–202.
Li, L., He, Z.L., Tfaily, M.M., Inglett, P., Stoffella, P.J., 2018. Spatial-temporal variations of dissolved organic nitrogen molecular composition in agricultural runoff water. Water Res. 137, 375–383.
Lin, Y., Wang, L., Xu, K., Huang, H., Ren, H., 2021. Algae Biofilm Reduces Microbe-Derived Dissolved Organic Nitrogen Discharges: performance and Mechanisms. Environ. Sci. Technol. 55 (9), 6227–6238.
Liu, Z., Zhou, C., Ontiveros-Valencia, A., Luo, Y.-H., Long, M., Xu, H., Rittmann, B.E., 2018a. Accurate O2 delivery enabled benzene biodegradation through aerobic activation followed by denitrification-coupled mineralization. Biotechnol. Bioeng. 115 (8), 1988–1999.
Liu, Z., Zhou, C., Ontiveros-Valencia, A., Luo, Y.H., Long, M., Xu, H., Rittmann, B.E., 2018b. Accurate O(2) delivery enabled benzene biodegradation through aerobic activation followed by denitrification-coupled mineralization. Biotechnol. Bioeng. 115 (8), 1988–1999.
Locher, H.H., Leisinger, T., Cook, A.M.J.T.B.j., 1991. 4-Sulphobenzoate 3,4-dioxygenase. Purification and properties of a desulphonative two-component enzyme system from Comamonas testosteroni T-2 274 (Pt 3), 833–842.
Lusk, M.G., Toor, G.S., 2016. Biodegradability and Molecular Composition of Dissolved Organic Nitrogen in Urban Stormwater Runoff and Outflow Water from a Stormwater Retention Pond. Environ. Sci. Technol. 50 (7), 3391–3398.
Martin, K.J., Nerenberg, R., 2012. The membrane biofilm reactor (MBfR) for water and wastewater treatment: principles, applications, and recent developments. Bioresour. Technol. 122, 83–94.
Martínez-Pascual, E., Jiménez, N., Vidal-Gavilan, G., Viñas, M., Solanas, A.M., 2010. Chemical and microbial community analysis during aerobic biostimulation assays of non-sulfonated alkyl-benzene-contaminated groundwater. Appl. Microbiol. Biotechnol. 88 (4), 985–995.
Motteran, F., Nadai, B.M., Braga, J.K., Silva, E.L., Varesche, M.B.A., 2018. Metabolic routes involved in the removal of linear alkylbenzene sulfonate (LAS) employing linear alcohol ethoxylated and ethanol as co-substrates in enlarged scale fluidized bed reactor. Sci. Total Environ. 640-641, 1411–1423.
Mungray, A.K., Kumar, P., 2008. Anionic surfactants in treated sewage and sludges: risk assessment to aquatic and terrestrial environments. Bioresour. Technol. 99 (8), 2919–2929.
Mungray, A.K., Kumar, P., 2009. Fate of linear alkylbenzene sulfonates in the environment: a review. Int. Biodeterior. Biodegradation 63 (8), 981–987.
Okada, D.Y., Delforno, T.P., Etchebehere, C., Varesche, M.B.A., 2014. Evaluation of the microbial community of upflow anaerobic sludge blanket reactors used for the removal and degradation of linear alkylbenzene sulfonate by pyrosequencing. Int. Biodeterior. Biodegradation 96, 63–70.
Osborne, D.M., Podgorski, D.C., Bronk, D.A., Roberts, Q., Sipler, R.E., Austin, D., Bays, J. S., Cooper, W.T., 2013. Molecular-level characterization of reactive and refractory dissolved natural organic nitrogen compounds by atmospheric pressure photoionization coupled to Fourier transform ion cyclotron resonance mass spectrometry. Rapid Commun. Mass Spectr. 27 (8), 851–858.
Pakou, C., Stamatelatou, K., Kornaros, M., Lyberatos, G., 2007. On the complete aerobic microbial mineralization of linear alkylbenzene sulfonate. Desalination. 215 (1–3), 198–208.
Perales, J.A., Manzano, M.A., Sales, D., Quiroga, J.M., 2003. Biodisposition of linear alkylbenzene sulphonates and their associated sulphophenyl carboxilic acid metabolites in sea water. Int. Biodeterior. Biodegradation 51 (3), 187–194.
Rittmann, B.E., 2006. The membrane biofilm reactor: the natural partnership of membranes and biofilm. Water Sci. Technol. 53 (3), 219–225.
Rittmann, B.E., 2007. The membrane biofilm reactor is a versatile platform for water and wastewater treatment. Environmental Engineering Research 12 (4), 157–175.
Rutere, C., Knoop, K., Posselt, M., Ho, A., Horn, M.A., 2020. Ibuprofen Degradation and Associated Bacterial Communities in Hyporheic Zone Sediments. Microorganisms 8 (8), 1245.
Sánchez-Peinado Mdel, M., González-López, J., Martínez-Toledo, M.V., Pozo, C., Rodelas, B., 2010. Influence of linear alkylbenzene sulfonate (LAS) on the structure of Alphaproteobacteria, Actinobacteria, and Acidobacteria communities in a soil microcosm. Environ. Sci. Pollut. Res. Int. 17 (3), 779–790.
Schleinitz, K.M., Schmeling, S., Jehmlich, N., von Bergen, M., Harms, H., Kleinsteuber, S., Vogt, C., Fuchs, G., 2009. Phenol degradation in the strictly anaerobic iron-reducing bacterium Geobacter metallireducens GS-15. Appl. Environ. Microbiol. 75 (12), 3912–3919.
Shaikh, I.N., Mansoor Ahammed, M., Sukanya Krishnan, M.P., 2019. In: Galanakis, C.M., Agrafioti, E. (Eds.), Sustainable Water and Wastewater Processing. Elsevier, pp. 19–54 (eds).
Stevens, H., Stübner, M., Simon, M., Brinkhoff, T., 2005. Phylogeny of Proteobacteria and Bacteroidetes from oxic habitats of a tidal flat ecosystem. FEMS. Microbiol. Ecol. 54 (3), 351–365.
Su, B., Liu, Q., Liang, H., Zhou, X., Zhang, Y., Liu, G., Qiao, Z., 2022. Simultaneous partial nitrification, anammox, and denitrification in an upflow microaerobic membrane bioreactor treating middle concentration of ammonia nitrogen wastewater with low COD/TN ratio. Chemosphere 295, 133832.
Swisher, R.D., 1986. Surfactant biodegradation. Surfactant Series, 2nd ed. Marcel Dekker, New York.
Tian, X., Zhao, J., Huang, J., Chen, G., Zhao, Y., 2021. The metabolic process of aerobic granular sludge treating piggery wastewater: microbial community, denitrification genes and mathematical model calculation. J. Environ. Chem. Eng. 9 (4), 105392.
Wang, J., Chu, L., 2016. Biological nitrate removal from water and wastewater by solid-phase denitrification process. Biotechnol. Adv. 34 (6), 1103–1112.
Wang, J., Liu, W., Luo, G., Li, Z., Zhao, C., Zhang, H., Zhu, M., Xu, Q., Wang, X., Zhao, C., Qu, Y., Yang, Z., Yao, T., Li, Y., Lin, Y., Wu, Y., Li, Y., 2018. Synergistic effect of well-defined dual sites boosting the oxygen reduction reaction. Energy Environ. Sci. 11 (12), 3375–3379.
Watanabe, T., Miura, A., Iwata, T., Kojima, H., Fukui, M., 2017. Dominance of Sulfuritalea species in nitrate-depleted water of a stratified freshwater lake and arsenate respiration ability within the genus. Environ. Microbiol. Rep. 9 (5), 522–527.
Wöhlbrand, L., Kallerhoff, B., Lange, D., Hufnagel, P., Thiermann, J., Reinhardt, R., Rabus, R., 2007. Functional proteomic view of metabolic regulation in "Aromatoleum aromaticum" strain EbN1. Proteomics. 7 (13), 2222–2239.
Wood, D.E., Lu, J., Langmead, B., 2019. Improved metagenomic analysis with Kraken 2. Genome Biol. 20 (1), 257.
Wu, H., Zhang, Q., Chen, X., Zhu, Y., Yuan, C., Zhang, C., 2022. The influence mechanism of DO on the microbial community and carbon source metabolism in two solid carbon source systems. Environ. Res. 206, 112410.
Zhang, L., Tang, C., Li, M., Wang, H., Zhang, S., Wang, J., Dong, X., Fang, D., Bai, H., Sun, Y., Yue, D., 2023. Identification of key surfactant in municipal solid waste leachate foaming and its influence mechanism. Water Res. 231, 119487.
Zhou, Y., Guo, B., Li, R., Zhang, L., Xia, S., Liu, Y., 2020b. Treatment of grey water (GW) with high linear alkylbenzene sulfonates (LAS) content and carbon/nitrogen (C/N) ratio in an oxygen-based membrane biofilm reactor (O2-MBfR). Chemosphere 258, 127363.
Zhou, Y., Li, R., Guo, B., Xia, S., Liu, Y., Rittmann, B.E., 2021a. The Influent COD/N Ratio Controlled the Linear Alkylbenzene Sulfonate Biodegradation and Extracellular Polymeric Substances Accumulation in an Oxygen-based Membrane Biofilm Reactor. J. Hazard. Mater. 422, 126862.
Zhou, Y., Li, R., Guo, B., Yu, N., Liu, Y., 2021b. Cometabolism accelerated simultaneous ammoxidation and organics mineralization in an oxygen-based membrane biofilm reactor treating greywater under low dissolved oxygen conditions. Sci. Total Environ. 789, 147898.
Zhou, Y., Li, R., Guo, B., Yu, N., Liu, Y.J.C., 2020c. Lumen Air Pressure (LAP) Affecting Greywater Treatment in An Oxygen-based Membrane Biofilm Reactor (O2-MBfR). Chemosphere 270, 129541.
Zhou, Y., Li, R., Guo, B., Zhang, L., Zou, X., Xia, S., Liu, Y., 2020a. Greywater treatment using an oxygen-based membrane biofilm reactor: formation of dynamic multifunctional biofilm for organics and nitrogen removal. Chem. Eng. J. 386, 123989.
Zhou, Y., Zhang, Z., Zhang, L., Xu, S., Guo, B., Liu, Y., Xia, S., 2019. Promoting waste activated sludge reduction by linear alkylbenzene sulfonates: surfactant dose control extracellular polymeric substances solubilization and microbial community succession. J. Hazard. Mater. 374, 74–82.